Structural Monitoring and Maintenance, *Vol. 12, No. 4 (2025) 377-393*
https://doi.org/10.12989/smm.2025.12.4.377

Quantitative scalar damage evolution of fire-exposed reinforced concrete beam using ultrasonic pulses

Gabriel I. Gamana*[1], Edgardo. S. Legaspi[1a],
Jordan. N. Velasco[2b] and John Lemar. M. Tirao[3c]

[1]*Department of Civil Engineering, Technological University of the Philippines, Manila, Philippines*
[2]*Department of Electrical Engineering, Pamantasan ng Lungsod ng Valenzuela, Philippines*
[3]*Department of Civil Engineering, Pamantasan ng Lungsod ng Valenzuela, Philippines*

(*Received July 18, 2024, Revised December 27, 2024, Accepted March 11, 2025*)

Abstract. Rapid urbanization worldwide drives the construction of numerous buildings and infrastructure, essential for both social and economic development. However, these structures face significant risks of partial or complete damage when exposed to accidental fires. While existing codes prioritize life safety measures, they often lack comprehensive guidelines for post-fire structural assessment and rehabilitation, potentially resulting in structural condemnation. This research study introduces an innovative approach utilizing the ultrasonic pulse velocity (UPV) test to develop a scalar damage model. This model correlates the damage parameter of reinforced concrete (RC) beams, both with and without fire exposure, to variables such as the nature and intensity of applied stresses, concrete strength, and steel ratio. The findings indicate a substantial reduction in initial UPV readings for RC beams exposed to fire, up to 20.51% compared to those without fire exposure, aligned with the existing literature suggesting a proportional loss in concrete strength. Moreover, the inclination angle of the elastic data trend is proportional to the damage accumulated by the concrete, notably higher for RC beams with fire damage, particularly under compression stress. Furthermore, this angle is also influenced by various factors, including the steel ratio and concrete strength, regardless of fire exposure. Additionally, RC beams subjected to fire damage exhibit reduced deflection, indicating a less ductile response compared to those without fire exposure. This reduced ductility is attributed to the decarbonization of the cement binder and the formation of crack networks in the concrete, leading to a decrease in overall response.

Keywords: fire damage; microcracks; scalar damage; ultrasonic pulses

1. Introduction

Concrete is one of the world's in-demand materials since urbanization is inevitable due to the advent of technological advancements. The United Nations (UN) estimates that in 2018, around 55% of the world's population was urbanized, and projected that by 2050, around 68% will live in

*Corresponding author, CE, M.Sc., E-mail: gabriel_gamana@tup.edu.ph
[a] CE, M.Sc., E-mail: edgardo_legaspi@tup.edu.ph
[b] EE, M.Sc., E-mail: ceit.velasco@gmail.com
[c] CE, BSCE, E-mail: ceit.tirao@gmail.com

 ISSN: 2288-6605 (Print), 2288-6613 (Online)

urbanized areas (United Nations 2019). Consequently, more buildings and infrastructure were built in the last decade, and this trend is expected to continue despite the effect of the COVID-19 Pandemic (International Monetary Fund 2021). Moreover, like any other materials that are subjected to deterioration, these structures face threats from super typhoons, earthquakes, as well as damage due to fire exposure, in the US alone around 368,500 residential buildings were exposed to confined and nonconfined fires as reported to the US Fire Department between 2017 to 2019 causing an estimated property loss of 8.1 billion US dollar (U.S. Fire Administration 2021). Hence, one of the challenges is that the current code provisions of fire design for building structures have been focused on ensuring life safety protection, thus providing sufficient time for the occupant to evacuate and for the firefighters to conduct the rescue operation. On the other hand, codes provide minimal consideration for post-fire structural assessment and rehabilitation, which could result in the structural condemnation of the building, and such an event would cause direct and indirect economic, historical, cultural, and environmental losses (Spinardi *et al*. 2017).

The temperature from the fire can reach beyond 1000ºC, which causes materials like concrete and steel to lose their strength and rigidity (Qin *et al*. 2022). The severity of fire damage is dependent on the temperature at which the structure was heated up and the duration of fire exposure. The strength of steel alone begins to decrease at around 350ºC, while a strength reduction between 30 to 40% was experienced at 500ºC. In addition, for the concrete material, dehydration of cement binder starts at 400ºC while decarbonization of the binder and formation of networks of cracks accompanied by rapid evaporation of water starts at around 700ºC (Stawiski 2006). Moreover, concrete strength reduction due to fire exposure is influenced by several variables such as member size, aggregate type, concrete porosity, load, and heat durations. Additionally, sudden temperature changes, especially when water at room temperature is poured into concrete at fire temperature, more specifically when the firefighters are extinguishing the fire, will lead to serious structural damage because of the excessive sudden contraction of concrete that will result in massive cracks. On the other hand, concrete in terms of fire protection is a great material as compared to wood and steel because of its low thermal conductivity and high specific heat capacity, one good illustration of its efficiency is demonstrated by the accidental fire that occurred at Grenfell Tower in 2017, the building was exposed to fire for about 60 hours continuously but still managed to avoid total collapsed (Qin *et al*. 2022). The main concern for the structures that stand still after the fire exposure is whether they need to be retrofitted or, in extreme cases, to be demolished and replaced, since building officials and structural engineers shall ensure that the buildings exposed to fire without total global collapse shall perform their function safely in accordance with the code. Furthermore, the action to be taken shall be based on a proper assessment of the fire damage by means of mapping the damage itself since fire exposure of the structural elements is not uniform, during the initial visual assessment of fire damage, regions of concrete with severe degradation are easily visible as compared to less damaged structural components that is why a more comprehensive assessment with the use of laboratory specimens and Nondestructive test (NDT) is highly advisable, this damage mapping shall optimize both the safety level and the most economical solution (Albrektsson *et al.* 2011).

1.1 Fire damage assessment

Reinforced concrete structures that were exposed to fire have a higher tendency of sufficient residual strength due to the superior fire-resistant characteristics of concrete as compared to other construction materials. On the other hand, heat exposure may lead to irreversible serviceability and

strength losses, which is why a proper assessment technique is necessary to identify suitable repair procedures to extend the lifespan of the fire-exposed structures (Agrawal et al. 2019). For the past decades, numerous kinds of research have been directed to quantify the residual strength of structures exposed to fire and determine their structural reliability. El-Hawary *et al*. (1996) studied the effect of fire damage on the flexural strength of reinforced concrete (RC) beam subjected to a temperature of 650ºC for the durations of 0, 30, 60, and 120 minutes and then cooled using water, the authors concluded that the RC beams exposed to higher duration experienced a dropped in compressive strength up to 73% with respect to Schmidt hammer test. Chen et al. (2009) published a paper where a full-scale RC column was subjected to fire with a duration of 120 and 240 minutes and then a cooling period of one month, the author concluded that the higher the time exposure to fire the greater the strength reduction in the load-bearing capacity which is in compliance with the study of El-Hawary et al. Moreover, the author observed that the deterioration in strength can be slowed down by the recovery of a hot-rolled reinforcement bar after cooling. In addition, the authors emphasized that more attention must be given to the deformation and stress redistribution of RC buildings exposed to fire, especially for earthquake loads.

The later researchers combined the experimental and numerical methods to quantify the residual strength of fire-exposed RC structures, Raouffard and Nishiyama (2016) studied the residual strength of RC frames after fire exposure using a two-dimensional finite element model, the author concluded that there is a 30% strength reduction to the laboratory specimen that was considerably predicted by the proposed numerical model. Moreover, Ioannou *et al*. (2017) published their research about the fragility assessment of RC structures based on the expert's judgment and created an initial fire damage scale for columns and slab to aid the design decision. This scale is derived from the damage state as developed by the Concrete Society. In addition, the authors recommended that further research must be directed to the determination of thresholds for other types of structural elements, as well as to study the local damage assessment of every structural element that could lead to the creation of a global damage scale to quantify the overall performance of the RC buildings exposed to fire. Naser and Salehi (2020) used machine learning to assess fire-induced concrete spalling that utilized the k-nearest neighbor (k-NN) and genetic programming (GP) to examine the 11 factors that influence concrete spalling, the authors concluded that among these factors compressive strength, section width, stirrup spacing, eccentricity, humidity, and load level greatly affects the spalling phenomenon. Furthermore, the author concluded that the applied techniques using sequential backward selection (SBS) predicted concrete spalling with an accuracy of 77% while the GP analysis successfully identified the fire-induced concrete spalling with an accuracy of 90%. In 2022, one of the most recent research is the implementation of a hybrid deep-learning network composed of a Convolution Neural Network (CNN) used as a crack feature extractor and a Long Short Term Memory (LSTM) network used as a crack detector to develop an autonomous macrocrack damage detection framework for RC buildings after fire exposure, the results showed that the hybrid CNN-LSTM network demonstrates superiority as compared to its predecessors in terms of crack pattern detection after it has been tested to real-time data, the hybrid network produces 99.15% accuracy, 99.02% precision, and 99.49% of recall, this impressive performance opens the opportunity to develop automated detection tools that will be used on-site in the future to improve the traditional visual inspection which is subjective and turn it into quantitative and automated scanning method that will minimize the impact of human error in the initial damage assessment (Diana Andrushia *et al*. 2022).

Ultimately, automation of visual inspection using artificial intelligence in combination with on-site NDT will be one of the most effective ways to map and quantify the residual strength of fire-

exposed RC structures. Meanwhile, this research focused on local damage assessment of an RC beam using the ultrasonic pulse velocity (UPV) under the Strut-and-Tie model condition or the so-called "D-region". As observed, the majority of the literature focuses on quantifying fire damage for the structural members, mainly classified under the continuity region or the so-called "B-region". These members follow the Bernoulli hypothesis, where the strain distribution is considered to be linear and the simplified theoretical assumptions are valid. On the contrary, this research studied the sections as discussed by Schlaich and Schafer, where nonlinear strain distribution occurs, such as near concentrated loads, bends, corners, openings, and other discontinuities or disturbances in detail (Schlaich and Schafer 1991). Hence, Gamana and Baccay (2022) published a study that demonstrates the inconsistency of members under the D-region with respect to the code-based assumptions, mainly in the line of the B-region, while studying the damage evolution of an RC beam using ultrasonic pulses. In continuation, this research compares the damage propagation of the ultrasonic pulses with respect to the concrete's elastic modulus for the controlled specimen and the fire-exposed RC beam. This approach demonstrates how damage accumulates and propagates for both conditions, considering the effect of the D-region and its implications for the residual strength of the RC beams.

1.2 Ultrasonic pulses

As technology advances, the systematic implementation of damage assessment for existing structures paved the way for the development of numerous types of Nondestructive tests (NDT). Unlike the conventional destructive testing that requires laboratory specimens, one of which is the so-called "core sampling" which provides a limited number of data since it can only be used for the area that is not critical for the structure to avoid weakening its structural integrity, this means that the result can be the representation of some of the portion of the structure but it does not give a complete understanding of the damage propagation itself due to its limited quantity. On the other hand, NDT offers an unlimited amount of data that can be applied to any point in the structure since it does not require any disruption to the material or interference with its function. NDT can be used to compare every structural element and to assess which of them has undergone severe mechanical degradation, so a proper repair solution can be applied (Collins *et al*. 2014).

Numerous NDTs have been developed and used for structural health monitoring; among these techniques UPV test has become one of the most popular because of its versatility in on-site applications and its relatively low cost (Nogueira and Rens 2018). Since 1938 when Powers first used the vibrational motion of sound waves to determine the material's mechanical properties (Powers 1938), tonnes of research has been directed toward the development of the now so-called "linear UPV test", some of its applications are Camara *et al*. (2019) published a paper showing that UPV can also be used to monitor the strength of self-healing concrete similar to conventional concrete, while most recently, Gamana and Baccay (2022) used UPV to create a damage model and concluded that the nature and intensity of the applied stress, steel reinforcement, and concrete strength greatly affect the damage evolution and propagation on an RC beam. Moreover, for the past decades, UPV has also been used to assess the mechanical degradation of concrete exposed to fire. Yang *et al*. (2009) used UPV to assess the residual strength of concrete subjected to elevated temperatures and concluded that concrete mix proportion does not significantly affect the concrete residual strength (Yang *et al.* 2009). In 2020, Wróblewski and Stawiski used UPV to assess the concrete structure exposed to real accidental fire and observed that the UPV test is more reliable when concrete porosity and placement direction were also considered (Wróblewski and Stawiski

2020). Meanwhile, Almasaeid (2024) used UPV to assess the concrete splitting strength exposed to elevated temperatures of up to 800ºC and incorporated an artificial neural network (ANN) to predict the residual splitting strength and concluded that at its highest temperature concrete losses up to 75% of its splitting strength while the ANN provided reasonable forecast with its coefficient of determination (R2) of 0.943. Furthermore, this research utilized the classical linear theory of elasticity for an isotropic medium to express the UPV readings in terms of the dynamic elastic modulus as shown in Eq. (1).

Where $\rho_{Conc.}$ is the concrete density, υ is the Poison's Ratio, V is the UPV reading, specifically the longitudinal wave, and E is the dynamic elastic modulus. In addition, the concrete density and Poison's ratio were assumed to be constants, so the damage propagation will manifest through the deviations of the elastic modulus. Meanwhile, to capture the decay of the mechanical property, this paper used the complementary parameter as introduced by Rabotnov and Leckie (1969), as shown in Eq. (2).

$$\rho_{Conc.}(V)^2 = \frac{E(1-\upsilon)}{(1+\upsilon)(1-2\upsilon)} \tag{1}$$

$$D = 1 - \frac{E_1}{E_0} \tag{2}$$

Where D is the damage parameter, E_1 is the dynamic modulus of elasticity, and E_0 is the undamaged elastic modulus. Thus, combining Eq. (1) and Eq. (2) gives the scalar damage variable based on the elastic modulus as shown in Eq. (3).

$$D = 1 - \left(\frac{V_1}{V_0}\right)^2 \tag{3}$$

Where V_1 is the UPV reading simultaneous with the load application, while V_0 is the UPV reading of the undamaged concrete. This research utilized the sensitivity of ultrasonic pulses to create scalar damage models that are based on the graph between the scalar damage parameter D and the flexural stress-strength ratio, a ratio between the ultimate stress experienced by the RC beam and the equivalent stress with respect to the corresponding value of the scalar damage variable.

2. Research methodology

2.1 Materials and specimens

The research methodology used fifty-four (54) RC beam specimens with three different concrete strengths which are commercially available such as 3000, 4000, and 5000 Psi while the amount of 20 mm flexural deformed reinforcement bars used five (5) different steel ratios such as 1.208%, 1.812%, 2.435%, 3.797%, and 5.150% as shown in Table 1. On the other hand, a 75 mm center-to-center fixed stirrups spacing that varies in diameter from 10 mm to 16 mm was also used as shown in Fig. 1, while three 54 kHz ultrasonic transducers that emit longitudinal waves were placed at three different locations to simultaneously monitor the ultrasonic pulses together with the center-point destructive flexural test as shown in Fig. 2. Half of the beam specimens were exposed to fire with a sustained minimum temperature of 910ºC for 60 minutes and cooled to room temperature for a minimum of 3 days before the destructive test, the fire was concentratedly

applied at the midspan using two fire torches In each face. This paper focuses on studying the effects of the nature and intensity of the applied stress, concrete strength, and steel ratio on the damage evolution and propagation of RC beams subjected to elevated temperature and under the condition of D-region.

2.2 Research instruments

The UPV devices used in this research are PUNDIT Lab+ with ultrasonic transducers that have a 54 kHz resonating frequency as shown in Fig. 3. The PUNDIT Lab+ is a flexible instrument

Fig. 1 Deformed Reinforcement Bar inside the beam mold

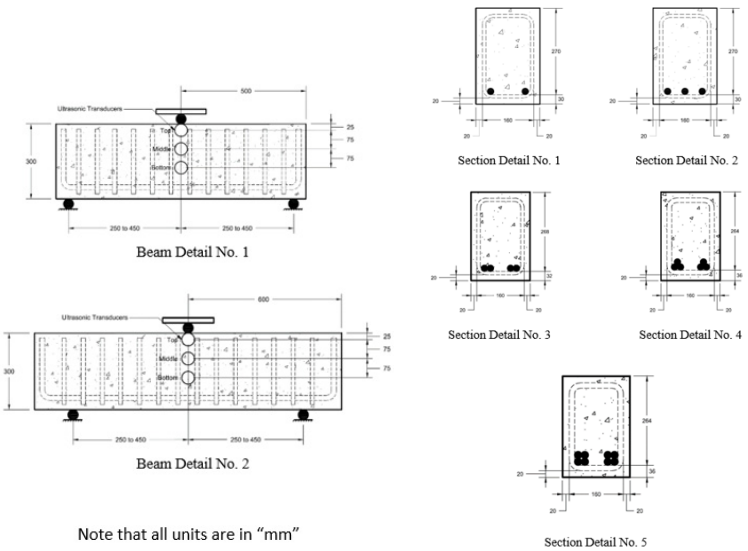

Fig. 2 Beam and Section Details

Table 1 Design Mix Proportion

Mix Design	A			B			C		
Compressive Strength (Psi)	3000			4000			5000		
No. of Main Rebar (Pcs)	2	3	4	3	4	6	4	6	8
Dia. of Stirrups Rebar (mm)	10	10	12	10	12	16	12	16	16
Section Detail	1	2	3	2	3	4	3	4	5
Beam Detail	1	1	1	1	1	1	1	1	2

Fig. 3 PUNDIT Lab+ with 54 kHz Ultrasonic Transducers

Fig. 4 RC beam inside the fabricated fire furnace

primarily designed for laboratory operations, it has a measuring resolution of 0.1 μs, a bandwidth of 20 to 500 kHz, a measuring range of 15 m, and using PROCEQ Punditlink software, it can be remotely controlled using computers with an oscilloscope function. Moreover, this device has a data logging function that eases the data gathering, export, and analysis using third-party software, which minimizes the errors in human interactions.

In addition, the settings of PROCEQ Punditlink software are as follows: the reading interval was set to one every second, with the event's number was set to 5000 which is the device's maximum since the time of which the RC beam's total global collapse is unknown, and the number of readings per event was set to one. Furthermore, for the advanced settings, the probe was set to 54 kHz based on the ultrasonic transducer's resonating frequency, while the correction factor due to temperature was set to 1.0, and the measuring resolution was set to 0.5 μs. Ultimately, the amplitude and Rx probe gain were both set to automatic, while for the whole process, the selected units for the length and strength were "m" and "MPa" respectively.

Fig. 5 Destructive flexural test of RC beam while simultaneously measuring the ultrasonic pulses

2.3 Research setup

The research methodology starts with two sets of RC beams, the first set represents the control specimen composed of beams without fire exposure while the second set are beams exposed to elevated temperatures reaching beyond 910ºC for 60 minutes using two fire torches per beam's face and enclosed by a fabricated wall to maintain the temperature as shown in Fig. 4, the beams were allowed to cool down with a minimum duration of 3 days before subjecting to destructive test. Moreover, prior to the research experiment, a functional check of the PUNDIT Lab+ and zero time adjustments were performed for proper calibration, while the direct transmission was used for the transducer setup with petroleum jelly as a coupling agent. Both sets of RC beams were placed on the ultimate testing machine (UTM) supported by the fabricated flexural attachment between two steel rods with a center-to-center distance ranging from 500 to 900 mm, with an overhang on both ends. The 54 kHz ultrasonic transducers were securely attached to the beam's face using a fabricated ultrasonic transducer holder made from plywood to ensure the continuous ultrasonic pulse reading while undergoing a destructive flexural test.

The measurement of ultrasonic pulses follows the instructions as prescribed by ASTM C597, the standard test method for pulse velocity through concrete, which requires the firm attachment of the ultrasonic transducers to generate a good transmission that can be verified by the PROCEQ Punditlink software when the pulse attenuation is 100%. Since the direct distance between two transducers was initially measured together with the abovementioned PROCEQ Punditlink settings, it will become the input for software to compute automatically the velocity of ultrasonic pulses as well as the decay of their pulse attenuation. Prior to the destructive test, an initial measurement of the UPV and pulse attenuation was conducted with a minimum of 20 readings per device, assuring that no zero readings occurred between the intervals, this is to capture the undamaged properties of the RC beam before loading. Moreover, the setup of the destructive flexural test follows the instructions as prescribed by ASTM C293, the standard test method for the flexural strength of concrete using a simple beam with center-point loading. Furthermore, ultrasonic pulses are simultaneously measured using the data logging mode of the UPV device together with the UTM load until RC beam failure, as shown in Fig. 5.

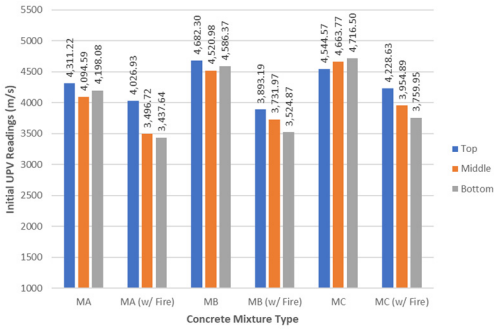

Fig. 6 Initial UPV reading to Concrete mixture type with and without fire exposure

3. Experimental results and discussion

Following the destructive flexural test while simultaneously measuring the ultrasonic pulses in three different locations until beam failure, consistent with the research methodology as aforementioned. This research studied the behavior of RC beams under the D-region exposed to elevated temperature and air-cooled for a minimum of three days, together with other variables such as intensity and nature of the applied stress, steel ratio, and concrete strength, where the results and interpretations are presented hereafter.

The subsequent discussions present the initial UPV readings of the concrete mixture with and without fire exposure as shown in Fig. 6. It can be observed that the bottom transducer experienced the largest reduction in UPV readings with an average of 20.51% as compared to the top and middle transducers with an average reduction of 10.13% and 15.75%, respectively. Both bottom and middle transducers accumulated larger fire damage as compared to the top transducer since the fire torches were placed directly to the bottom and near the middle transducer, making the temperature from these locations beyond 900ºC while quite less for the top transducer, these findings are aligned with the literature as mentioned earlier that concrete exposed to a higher temperature will experience higher fire damage due to dehydration and decarbonization of cement binders in addition to rapid evaporation of water that leads to the formation of cracks networks. Moreover, based on the initial UPV reading without stress application, there is no significant relationship that exists with respect to the concrete strength and steel ratio, which is also consistent with the study of Yang *et al.* (2009).

Meanwhile, Fig. 7(a) presents the UPV Readings to the Flexural Stress-Strength ratio of the RC beam without fire damage, while Fig. 7(b) presents the RC beam with fire damage; the trends as observed in these figures are consistent with the eight other average graphs that exhibit the same trends. It is observed that for both conditions the degradation of the top transducer starts at lower stress levels such as 72% for the beam without fire damage while 54% for the beam with fire damage as compared to the middle and bottom transducers where drastic deterioration normally starts beyond 80% stress level, this signifies that with respect to the nature of stress, concrete under compression accumulates severe damage as compared to the concrete under tension at earlier stress, this result is counter-intuitive since the author expects that concrete under tension will be the first to show damage since concrete is much weaker in tension than in compression stress.

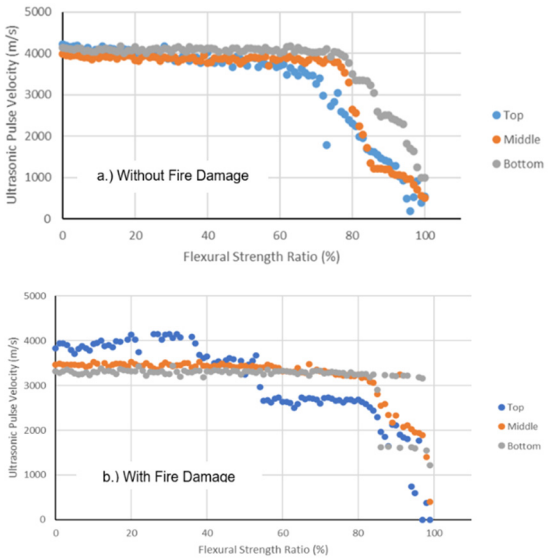

Fig. 7 UPV Readings to Flexural Stress-Strength ratio of RC Beam (RC-S-MA-T1)

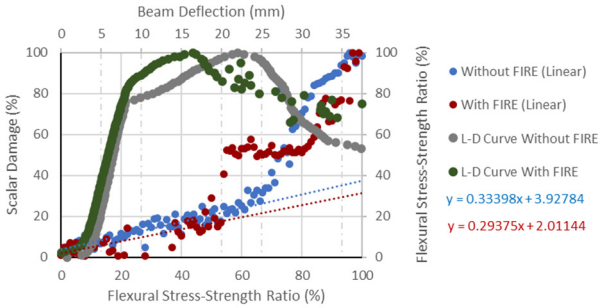

Fig. 8 Scalar Damage and Beam Deflection to Flexural Stress-Strength ratio of RC Beam (RC-S-MA-T1)

Hence, this phenomenon might be the effect of the research setup since the beam is under the discontinuity region where, instead of failing under the pure flexure, an internal strut develops in the concrete that directly transfers the forces to the reinforcement that served as the tension member to maintain equilibrium, commonly known as the "Strut-and-tie model". In addition, both top and middle transducers are subjected to compression stresses, with the middle transducer exposed to higher fire damage than the top transducers, as shown in Fig. 6.

On the other hand, top transducers who are exposed to higher applied stress show early signs of deterioration in comparison to middle transducers which is 72% as compared to 77% for the beam without fire damage and 54% to 83% for the beam with fire damage, respectively, which serve as evidence that regardless of the amount of initial damage due to fire exposure, concrete under higher compression stress will be a reliable point within the structure to monitor the amount of damage as well as to predict the possible residual strength of the structural component. Moreover,

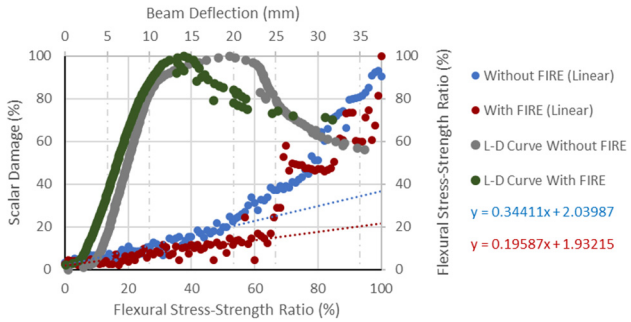

Fig. 9 Scalar Damage and Beam Deflection to Flexural Stress-Strength ratio of RC Beam (RC-S-MA-T2)

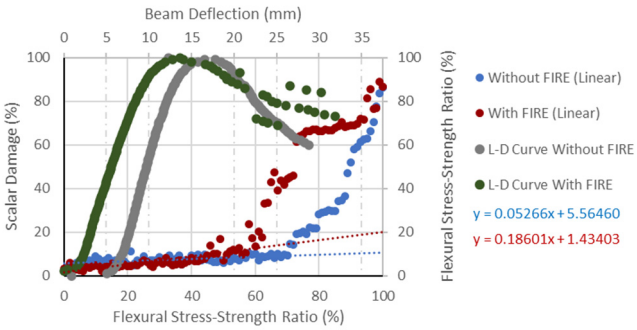

Fig. 10 Scalar Damage and Beam Deflection to Flexural Stress-Strength ratio of RC Beam (RC-S-MA-T3)

comparing the beams with and without fire exposure, the top transducer becomes even more significant since for the majority of the beam with fire damage, the transducers at compression showed mechanical degradation at lower stress levels such as 54%, 69%, and 63% as compared to the top transducers of the same beam without fire damage such as 72%, 81%, and 89%. This is consistent with the literature that concretes exposed to fire accumulate damage from the exposure; hence, the early deterioration of UPV readings is the manifestation of damage induced to the concrete by fire exposure. On the other hand, comparing the actual ultimate moment of both beams, with and without fire exposure it is observed that there is no significant difference between the two, even though the reinforced concrete beam suffers damage due to elevated temperature since the rebar already recovered its strength when the temperature cooled down to room temperature which is consistent also with the literature. Furthermore, after the flexural destructive test, among the ultrasonic transducers placed at three different locations, the top, which is under compression stress, becomes the most important since it shows sensitivity to damage propagation as compared to the middle and bottom, consistent with the study conducted by Gamana and Baccay (2022). Therefore, the graphs shown hereafter focus on comparing the top transducers of both sets of specimens together with the flexural stress-strength ratio as well as the load-deflection curve of the RC beam.

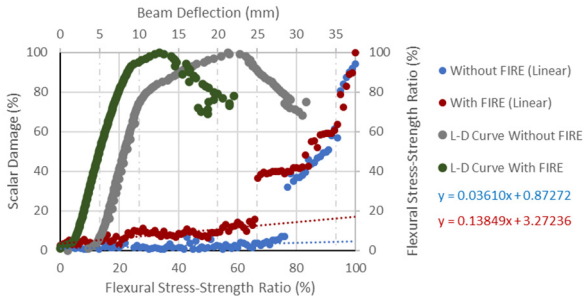

Fig. 11 Scalar Damage and Beam Deflection to Flexural Stress-Strength ratio of RC Beam (RC-S-MB-T1)

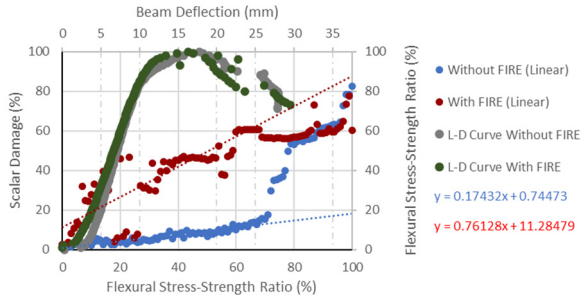

Fig. 12 Scalar Damage and Beam Deflection to Flexural Stress-Strength ratio of RC Beam (RC-S-MB-T2)

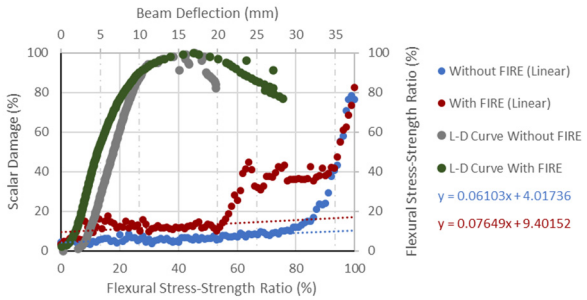

Fig. 13 Scalar Damage and Beam Deflection to Flexural Stress-Strength ratio of RC Beam (RC-S-MB-T3)

Figs. 8-16 presents the relations of scalar damage to flexural stress-strength ratio, stress intensity, nature of stress, and steel ratio for concrete mixtures A, B, and C. The aforementioned beam specimens have steel ratios of 1.208%, 1.812%, 2.435%, 3.797%, and 5.150% where each scalar damage graph is divided into two sets of data trends as shown in the figures such as linear regression which normally ranges from 0 to 50% stress level and nonlinear regression which is normally beyond 50% stress level. The data of linear regression shows a linear relationship

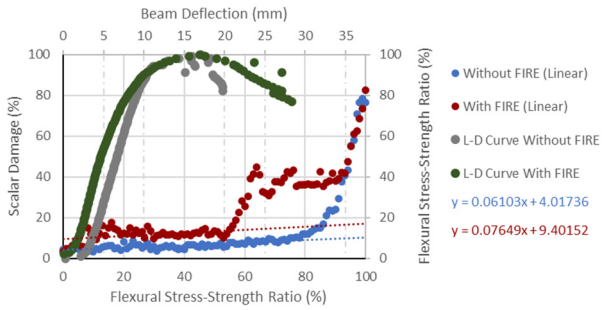

Fig. 14 Scalar Damage and Beam Deflection to Flexural Stress-Strength ratio of RC Beam (RC-S- MC-T1)

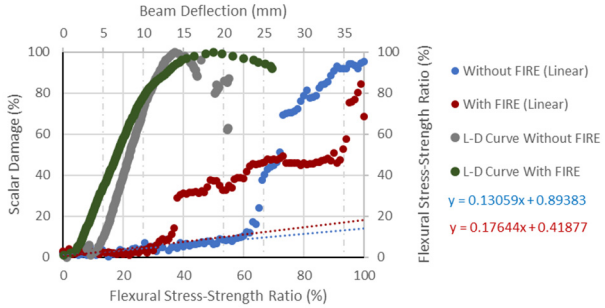

Fig. 15 Scalar Damage and Beam Deflection to Flexural Stress-Strength ratio of RC Beam (RC-S- MC-T2)

Figs. 8-16 presents the relations of scalar damage to flexural stress-strength ratio, stress intensity, nature of stress, and steel ratio for concrete mixtures A, B, and C. The aforementioned monitor for early detection of mechanical damage. The data of nonlinear regression shows a trend in rupture, where UPV readings decrease significantly due to heavy damage to the beam's section. This damage occurs in the plastic region where stress redistribution leads to the formation of plastic hinges. At this stage, macrocracks are formed as a result of the accumulation of microcracks, leading to visible and irreversible damage.

Consequently, the inclination angle of the linear regression was used to monitor the rate of damage accumulation of the specimen since this parameter is proportional to the deviations of UPV reading as the stress level increases. Hence, two-thirds of the average sample showed that the inclination angle of the top transducers for the beams with fire damage is larger such as 10.537°, 7.885°, 37.281°, 4.374°, 14.059°, and 10.006° as compared to the beam without fire damage with 3.014°, 2.067°, 9.888°, 3.492°, 8.036°, and 7.440° for Figs. 10-15, respectively. The RC beam with fire exposure accumulates a larger inclination angle because the concrete was exposed to fire that induced initial damage before the load was placed, this implies that the RC beam with fire exposure has the highest rate of deterioration as compared to the RC beam without fire exposure which is aligned with earlier observations with regard to UPV readings, the deviation of inclination angle represents microstructural degradation detected using ultrasonic pulses and

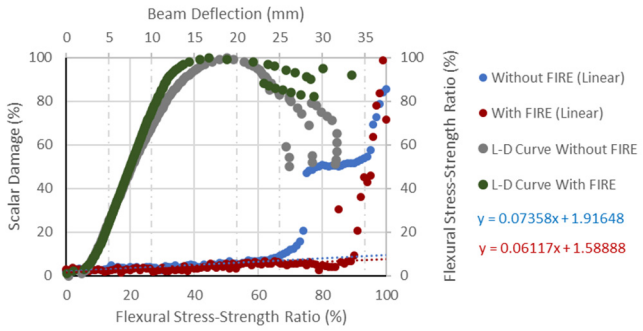

Fig. 16 Scalar Damage and Beam Deflection to Flexural Stress-Strength ratio of RC Beam (RC-S- MC-T3)

further magnified by the scalar damage formula to monitor the concrete's degradation prior to the formation of macrocrack defects. Moreover, fire exposure makes the RC beam response less ductile as shown in the beam's deflection at maximum loadings such as 16.427 mm, 14.099 mm, 12.802 mm, 12.613 mm, 16.249 mm, 16.892 mm, 14.700 mm, 18.741 mm, and 16.707 mm for the beam with fire exposure while 22.014 mm, 19.550 mm, 16.585 mm, 21.333 mm, 17.728 mm, 17.135 mm, 15.974 mm, 13.902 mm, and 18.842 mm for beams without fire exposure for the Figs. 8-16, respectively. Although the RC beam did not significantly lose its strength due to fire exposure since the ultimate moments of both sets are still numerically close to one another as mentioned earlier, it becomes evidently visible that it does become less ductile since the deflection at the ultimate load is smaller, it implies that it will reduce the visibility of damage for the occupants before the total global collapse of the structural component with fire exposure.

In summary, Figs. 8-16 illustrates the relationship between the steel ratio and the slope of the elastic data trend. As the amount of steel reinforcement increases, the slope decreases. For instance, beams exposed to fire under concrete mixture A show inclination angles of 16.370°, 11.082°, and 10.537° with steel ratios of 1.208%, 1.812%, and 2.435% respectively. Similarly, beams exposed to fire under concrete mixture B exhibit angles of 7.885° and 4.374° with steel ratios of 1.812% and 3.797% respectively. For concrete mixture C, angles are 14.059°, 10.006°, and 3.500° with steel ratios of 2.435%, 3.797%, and 5.150% respectively. Moreover, the effect of the nature of the applied stress is significantly affected by the amount of reinforcement as observed, data showed that the transducers under compression stress deteriorate earlier as compared to transducers under tension since the concrete under tension stress starts to deteriorate consequent to rebar yielding as shown in Fig. 7. Although the concrete under compression stress deteriorates earlier, the concrete under tension drastically deteriorates at a higher stress level after the rebar yielding, as shown in the steep slope of the bottom data series. Furthermore, the additional reinforcement bar stiffened the concrete's response to tension stresses where the bottom transducers were placed, since the drastic deterioration of the bottom transducer becomes even closer to ultimate strength as the steel ratio increases. This additional stiffness is also shared for the concrete compression part, where the top and middle transducers were attached. This behavior is a brittle response and critical since there is no warning prior to the sudden collapse. Furthermore, this research reinforced the American Concrete Institute (ACI) code principles that limit the amount of steel ratio to assure the beam's ductility to the applied load.

In Figs. 8-16, the correlation between concrete strength, scalar damage, and flexural stress-strength ratio is clearly depicted. Figs. 9 and 11 compare concrete mixtures A and B at a steel ratio of 1.812%, while Figs 10, 12, and 14 compare mixtures A, B, and C at a steel ratio of 2.435%. In contrast, Figs 13 and 15 compare mixtures B and C at a steel ratio of 3.797%. These figures demonstrate that concrete strength influences damage propagation: higher concrete strength leads to earlier significant deterioration of the scalar damage variable relative to the flexural stress-strength ratio, with a decrease in the inclination angle. This behavior is attributed to the brittle nature of concrete, constrained by a strain limitation of 0.003, as discussed in the literature. Despite increased beam capacity with higher concrete strength, the strain limit occurs at lower stress levels, indicating a reciprocal relationship between concrete strength and strain limitation.

4. Conclusions

Based on the results of the study, the following conclusions were drawn:

- The UPV measurement of the RC beam exposed to fire damage decreases compared to the one without fire damage. Consequently, the bottom transducer, which was exposed to the highest temperature, shows the greatest decrease in UPV reading. This aligns with existing literature indicating that as concrete endures higher temperatures, it loses strength because of cement binder dehydration and decarbonization, along with rapid water evaporation, which leads to the formation of crack networks.
- The angle of the elastic data trend varies depending on the intensity of the applied stress. Analysis of the data reveals that transducers positioned at various points show varying rates of degradation in the scalar damage parameter. As stress intensity increases, so does the angle of inclination. Moreover, RC beams subjected to fire exhibit larger inclination angles in addition to their greater degradation at lower stress levels as compared to the RC beam without fire exposure, indicating the pivotal role of initial damage to the beam under elastic and plastic regions.
- The nature of the stress applied influences the angle of inclination in the elastic data trend, irrespective of whether the RC beam has been exposed to fire damage initially. From the collected data, it is evident that concrete subjected to compressive stress exhibits a higher inclination angle compared to that under tension. Furthermore, the scalar damage parameter at the transition of the data trend for transducers experiencing tension stress deteriorates significantly at higher stress levels compared to those under compression stress, attributed to rebar yielding.
- The inclination angle of the elastic data trend is influenced by the steel ratio, regardless of whether the RC beam has encountered fire damage beforehand. As the steel ratio increases, the inclination angle of the elastic data trend decreases. Analysis of the observed data aligns with the UPV readings, indicating that additional steel reinforcement enhances the concrete's resistance to tensile stresses. This increased stiffness also extends to the concrete under compression.
- The elasticity data trend's angle of inclination is influenced by the strength of the concrete, regardless of whether the RC beam has experienced fire damage previously. It has been noted that the inclination angle decreases with higher concrete strength. This observation is in line with the findings from UPV readings, which suggest that the concrete's brittleness and its strain limitations contribute to this trend.
- The ductile behavior of RC beams is affected by the initial fire damage. It has been noticed that

the deflection of RC beams subjected to fire damage is lower compared to those without fire exposure. This is attributed to the decarbonization of the cement binder and the development of a network of cracks in the concrete, which reduces its strength and consequently impacts the overall response of the RC beam.

Acknowledgments

The authors are grateful to the administration of the Technological University of the Philippines, Manila, and the Pamantasan ng Lungsod ng Valenzuela for allowing the researchers to conduct their laboratory investigations in their research centers.

References

Agrawal, A. and Kodur, V.K.R. (2019), "A novel experimental approach for evaluating residual capacity of fire damaged concrete members", *Fire Technol*., **56**, 715-735, https://doi.org/10.1007/s10694-019-00900-1.

Albrektsson, J., Flansbjer, M., Lindqvist, J.E. and Jansson, R. (2011), "Assessment of concrete structures after fire", SP Technical Research Institute of Sweden, 19, 3-93.

Almasaeid, H. (2024), "Ultrasonic pulse velocity and artificial neural network prediction of high-temperature damaged concrete splitting strength", *Appl. Sci*., **6**(4), https://doi.org/10.1007/s42452-024-05645-3.

Camara, L.A., Wons, M., Esteves, I.C.A. and Medeiros-Junior, R.A. (2019), "Monitoring the self-healing of concrete from the ultrasonic pulse velocity", *J. Compos. Sci*., **3**(1), https://doi.org/10.3390/jcs3010016.

Chen, Y.H., Chang, Y.F., Yao, G.C. and Sheu, M.S. (2009), "Experimental research on post-fire behaviour of reinforced concrete columns", *Fire Saf. J*., **44**, 741-748. https://doi.org/10.1016/0950-0618(95)00041-0.

Collins, J., Mullins, G., Lewis, C. and Winters, D. (2014), "State of the practice and art for structural health monitoring of bridge substructures", US Department of Transportation, Federal Highway Administration.

Diana Andrushia, A., Anand, N., Mary Neebha, T., Naser, M.Z. and Lubloy, E. (2022), "Autonomous detection of concrete damage under fire conditions", *Automat. Constr*., **140**(104364), https://doi.org/10.1016/j.autcon.2022.104364.

El-Hawary, M., Ragab, A., El-Azim, A. and Elibiarif, S. (1996), "Effect of fire on flexural behavior of RC beams, *Constr. Build. Mater*., **10**(2), 147-150. https://doi.org/10.1016/0950-0618(95)00041-0.

Gamana, G. and Baccay, M. (2022), "Scalar damage modeling of reinforced concrete beam under polarized monotonic stress field using ultrasonic pulses", *Int. J. Adv. Sci. Eng. Inform. Tech*., **12**(4), 1526-1535. https://doi.org/10.18517/ijaseit.12.4.16518.

International Monetary Fund (2021), "World economic outlook: Recovery during a pandemic—health concerns, supply disruptions, price pressures", International Monetary Fund, Research Department, Washington, DC.

Ioannou, I., Aspinall, W., Rush, D., Bisby, L. and Rossetto, T. (2017), "Expert judgement-based fragility assessment of reinforced concrete buildings exposed to fire", *Reliab. Eng. Syst. Saf*., **167**, 105-127. https://doi.org/10.1016/j.ress.2017.05.011.

Naser, M.Z. and Salehi, H. (2020), "Machine learning-driven assessment of fire-induced concrete spalling of columns", *ACI Mater. J*., **167**, 105-127. https://doi.org/10.14359/51728120.

Nogueira, C.L. and Rens, K.L. (2018), "Effect of acoustoelasticity on ultrasonic pulses and damage of concrete under tensile stresses", *ACI Mater. J*., **115**(3), 381-392. https://doi.org/10.14359/51702184.

Powers T. (1938), "Measuring Young's modulus of elasticity by means of sonic vibrations", *Proc. ASTM*, **38**(2), 460-467.

Qin, D., Gao, P., Aslam, F., Sufian, M. and Alabduljabbar, H. (2022), "A comprehensive review on fire damage assessment of reinforced concrete structures", *Case Stud. Constr. Mater*., **16**(e00843), https://doi.org/10.1016/j.cscm.2021.e00843.

Rabotnov, Y.N. and Leckie, F.A. (1969), "Creep problems in structural members", John Wiley & Sons Inc.

Raouffard, M.M. and Nishiyama, M. (2016), "Residual load bearing capacity of reinforced concrete frames", *J. Adv. Concrete Technol*., **14**, 625-633. https://doi:10.3151/jact.14.625.

Schlaich, J. and Schafer, K. (1991), "Design and detailing of structural concrete using strut-and-tie models", *Struct. Engineer*, **69**(6), 113-125.

Spinardi, G., Bisby, L. and Torero, J. (2017), "A review of sociological issues in fire safety regulation", *Fire Technol*., **53**, 1011-1037. https://doi.org/10.1007/s10694-016-0615-1.

Stawiski, B. (2006), "Attempt to estimate fire damage to concrete building structure", *Arch. Civil Mech. Eng*., **6**(4), 23-29. https://doi.org/10.1016/S1644-9665(12)60273-8.

U.S. Fire Administration (2021). "Residential building fires (2017-2019)", Topical Fire Report Series, **21**(2).

United Nations (2019), "World urbanization prospects: The 2018 revision", United Nations, Department of Economics and Social Affairs, Population Division, New York.

Wróblewski, R. and Stawiski, B. (2020), "Ultrasonic assessment of the concrete residual strength after a real fire exposure", *Buildings*, **10**(154), https://doi.org/10.3390/buildings10090154.

Yang, H., Lin, Y., Hsiao, C. and Liu, J.Y. (2009), "Evaluating residual compressive strength of concrete at elevated temperatures using ultrasonic pulse velocity", *Fire Saf. J*., **44**, 121-130. https://doi.org/10.1016/j.firesaf.2008.05.003.

SN